



Three-Dimensional Mesoscopic Modelling of Concrete Confined by FRP Under Static and Dynamic Loading

Nyembo Ya Lumbu Lars and Jinhua Zhang^(✉)

School of Civil Engineering, Southeast University, Nanjing 210096, China
{larslumbu, zhangjh}@seu.edu.cn

Abstract. The strengthening of concrete materials has become one of the most important aspects in the design of any civil engineering structure, leading to a number of research to investigate and improve its mechanical behavior. The purpose of this study is to investigate the mechanical behavior of concrete confined with fiber reinforced polymer (FRP) under static and dynamic loading using a simple and thorough method. Two identical mesoscale concrete specimens and one FRP layer were created (concrete cylinder with a diameter of 50 mm, a depth of 100 mm, and the FRP layers with 1.27 mm of thickness) to compare the Finite element results to those of an existing experiment and a similar study previously conducted. The mechanical behavior of the simulated confined and unconfined concrete was compared to the mechanical behavior of an experiment with the same specimen size ratio. The localized phenomena in each element were considered in order to investigate the overall reaction of the created specimens, driven by the fact that concrete is a heterogeneous material made up of coarse particles, ITZ (Interfacial Transition Zone), and mortar. The parameters such as unconfined strength of concrete, maximum tensile, and maximum confinement stress are determined utilizing the confining pressure generated by the wrapped Fiber Reinforced Polymer on the three-dimensional mesoscopic concrete model based on the concrete-to-FRP confinement mechanism. From the findings of the investigation carried in this work, it is demonstrated that this study provides substantial insights into the question of strengthening and improving the mechanical behavior of concrete specimens subjected to static and dynamic loading.

Keywords: EASEC-17 · Singapore · Mesoscopic modelling · Concrete · Confining pressure · Mechanical property · Fiber reinforced polymer

1 Introduction

1.1 Mesoscale Modelling of Concrete Confined by FRP

With the fast growth of civil engineering infrastructure and military facilities, the requirement for improved engineering structure performance has constantly increased. As one of the most frequently and widely used building materials, concrete's mechanical qualities have garnered widespread interest from experts worldwide. Apart from the static

stresses that must be considered during structural design, the majority of structures are susceptible to strong dynamic loads such as collision, explosion, and penetration. As a result, a thorough examination of the static and dynamic behavior of concrete is critical (Wu et al. 2021a).

Concrete is a composite material that requires an explicit representation of its heterogeneous composition to understand the initiation and evolution of localized phenomena like damage and fracture (Wang et al. 2019). Coarse aggregates, mortar (cement with sand and fine aggregates embedded), and ITZ (Interfacial Transition zone) are the ingredients of concrete at the longest length scale with observable heterogeneities, referred to as the meso-scale (Wang et al. 2019). Based on a mesoscale understanding of the heterogeneous structure of concrete, a micromechanical model capable of predicting the fracture process of concrete is proposed and used to investigate the fracture parameters of concrete under uniaxial or biaxial loading (Wu et al. 2021a). As a result, many additional materials have been investigated to enhance and increase the concrete's resistance to dynamic and static loads. One of the approaches demonstrated in this article is the confinement of FRP materials using a cylindrical concrete specimen. Fiber reinforced polymer (FRP) composite materials have been used to strengthen concrete structures since the early 1990s, and the technique is now widely used around the world (Wang et al. 2019). Fiber Reinforced Polymer composites have a wide range of applications as a concrete confining material, including seismic retrofitting of existing reinforced concrete columns and the construction of concrete-filled Fiber Reinforced Polymer tubes as earthquake-resistant columns in new construction (Li et al. 2011). This article also looks at the use of Glass Fiber Reinforced Polymer material.

1.1.1 Material and Finite Element Modeling

The mesoscale concrete specimen (Mortar, Aggregate, and ITZ) was modeled and created in Ansys using the mesoscopic modeling approach as shown in Fig. 1. An additional material known as Glass Fiber Reinforced Polymer is modeled in LS DYNA in order to further investigate and strengthen the behavior of mesoscale concrete. Glass fiber reinforced polymer composites are manufactured in a variety of ways and are widely employed in a wide variety of applications. Initially, the ancient Egyptians utilized glass fibers extracted from heat softened glass to create vessels (Sathishkumar et al. 2014).

The GFRP layer wrapped around the mesoscopic concrete is modeled as a shell element with a thickness to the scale of 1 mm and the height of 100 mm to match that of the mortar matrix. LS DYNA is one of the most sophisticated finite element software packages available, and it comes with a wide library of composite materials to use in your simulations. In this study, the orthotropic materials behavior of unidirectional layers in composite shell constructions, which can be characterized by MAT054/055, is studied, as well as other related topics. Chang-Chang matrix failure criterion is used as the failure type in this simulation. The FRP-Concrete bond behavior was investigated using the *TIED_NODE_TO_SURFACE_OFFSET key card.

Coarse Aggregate Material Model The behavior of concrete aggregate stress–strain and damage function have been studied extensively in recent years (Wu et al. 2021a). For the concretes simulated in this study, coarse aggregate is considered more elastic

than mortar (Forti et al. 2020). Various studies have used elastic modulus and Poisson's ratio to simulate aggregate mechanical properties under quasistatic loads (Wu et al. 2021a). While creating materials models for mesoscale modelling, various mechanical and physical properties of concrete were taken into account (Wu et al. 2021a). This is because aggregates are not elastic under high strain rates (Wu et al. 2021a).

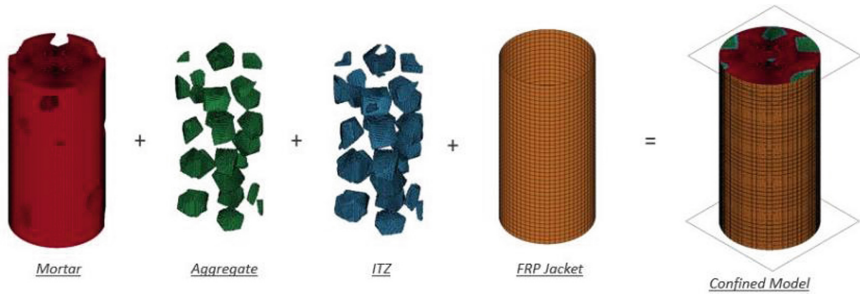


Fig. 1. Mesoscopic specimen and FRP layer

Ciment Mortar Material Model A common elastoplastic substance is mortar. Both compression and tension depict softening behavior in distinct ways. Compression is done through a damage. Tension may be relieved by the usage of cohesive cracks (Wu et al. 2021a). When it comes to simulating mortar matrix using the K&C model is an excellent choice to examine the tensile, shear, and compressive behavior of the material. Several researchers have used it.

ITZ Material Model The weakest connection between the aggregate and the mortar matrix is the Interfacial Transition Zone (ITZ). ITZ's properties are not entirely known, however its significant heterogeneity and high porosity and lower strength than mortar are well-accepted characteristics (Zhou and Hao 2008). ITZ has an elastic modulus of 50–70% of that of mortar (Shuguang and Qingbin 2015). As a conclusion, the comparable ITZ strength may be reduced to 75% of mortar, which has been identified and utilized in mesoscale models to capture the mechanical features of the ITZ phase (Wu et al. 2021a). K&C model was used for static compression stress-strain relationship and failure behavior of concrete. A 3D random mesoscale model and the K&C material model have been used to simulate and study ITZ failure patterns as well as their effects on the dynamic characteristics of concrete in previous research by Zhang et al. (Wu et al. 2021a).

1.2 Static Test

1.2.1 Load and Boundary Conditions

Numerical simulation relies heavily on the use of load and boundary conditions. LS Dyna's compression test machine simulates a realistic environment by applying BOUNDARY SPC on the specimen's top and bottom, representing the platens along

the compression axis. Using the Boundary Prescribed Motion Key Card, a compression Load was generated as a displacement on the specimen's top, while the specimen's bottom and FRP are constrained in all directions. Static compression is performed on both confined and unconfined mesoscopic concrete specimens in LS Dyna. First, the mechanical behavior of an unconfined cylindrical concrete specimen with a diameter of 50 mm and a height of 100 mm as shown in Fig. 1 is analyzed and compared to that of a confined cylindrical concrete specimen in the following section.

1.3 SHPB Simulation Test

To assess the dynamic compressive strength of (FFRP) Flax Fiber Reinforced Polymer confined concrete, a split Hopkinson pressure bar system with a diameter of 106 mm was generated in Ls dyna. As shown in Fig. 3, this setup consists of an 848 mm long projectile, a 7060 mm long incident bar, and a 4240 mm long transmission bar. The mesoscopic concrete specimen used in this simulation has a diameter of 100 mm and a height of 54 mm, while the wrapped FRP jacket has a thickness of 0.135 and 0.405 mm and an elastic modulus of 788 MPa Fig. 2(c). Both the incident and transmitted bars were modelled with elastic properties, with densities and elasticity modulus of 7800 kg/m³ and 210 GPa, respectively, to facilitate the propagation of the stress wave effect from the projectile impact to the specimen. Because the coast of the simulation was enormous when using the wave velocity used in the experiment conducted by (Bai et al. 2021), lowering the wave velocity and increasing the modulus of elasticity of the bars led to a significant shorter simulation run time. The strain rates investigated during the SHPB experiments were used to calculate the wave velocities used in this simulation (Bai et al. 2021). The mesoscale concrete specimen was inserted in between transmission and incident bars Fig. 2(a), and the contact nodes-segments between the specimen and the bars were also defined to simulate the stress wave from the incident bar to the transmission bar through the specimen. Two sensors were installed on the incident and transmission bars, respectively, at 3300 and 2800 mm from the specimen's ends as shown in Fig. 3.

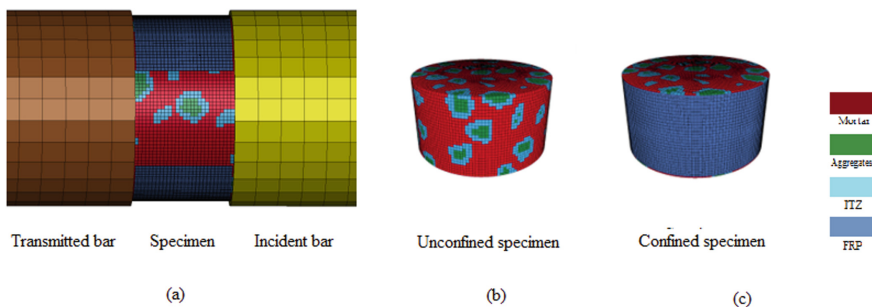


Fig. 2. Mesoscopic concrete specimen for dynamic analysis; (a) confined by FRP in the SHPB system (b) Unconfined specimen (c) confined specimen

2 Numerical Simulation Results

As we all know, the mechanical behavior of composite materials is significantly controlled by the unique qualities of their basic components, as well as the bonding strength of their transition zone (Wu et al. 2021b). The primary goal of this research is to determine the mechanical characteristics and failure factors of different kinds of composite materials. This article compares the findings of two kinds of mesoscale concrete models, confined and unconfined, investigated using uniaxial static and SHPB Dynamic compression tests. The type of FRPs used are GFRP for static compression analysis and flax FRP for dynamic analysis. In Table 1, L and D, are in mm, D/L is the ratio of the used bars.

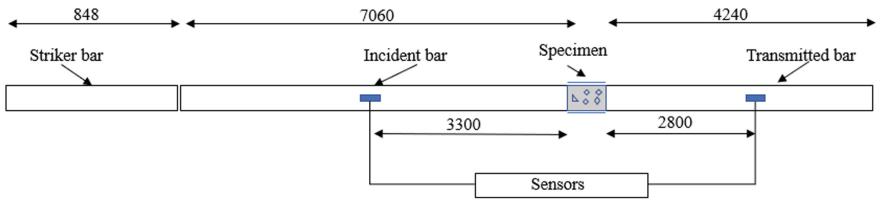


Fig. 3. SHPB setup for numerical simulation (mm)

Table 1. Size ratio of SHPB set up for numerical simulation

	Experiment setup				FEM setup			
	L mm	D mm	D/L	Sensor location mm	L mm	D mm	D/L	Sensor location mm
Striker	600	75	0.125	–	848	106	0.125	–
Incident bar	5000	75	0.015	2340	7060	106	0.015	3300
Transmitted bar	3000	75	0.025	2000	4240	106	0.025	2800
Specimen	38	70	1.85	–	54	100	1.85	–

2.1 Concrete’s Mechanical Reaction to Static Loading

The concrete models explored in this study have equivalent material properties and are subjected to the same loading situation for better simulation results observation and validation. In addition to the peak stress modelling and observation, an identical element is selected to study the optimal mechanical behavior of the constituent materials in both confined and unconfined specimens. Figure 4 shows the stress propagation in the unconfined concrete specimens. As noted above that concrete’s ingredients have an influence on the simulated results. Each constituents have their mechanical property. Since the ITZ is the weakest part of a concrete specimen, after loading the stress propagation and fractures patterns are noticed along the ITZ and aggregates as indicated in Figs. 4 and 5.

In the case of the confined concrete, the contact between the external part of the concrete specimen with wrapped FRP layer jacket create a passive pressure that is perpendicular to the compression axis. Considering the mechanical properties of Glass fiber reinforced polymer. The binding strength provided by the tight connection between concrete and FRP produces a strengthening mechanism (Eqs. 1–3) that improve the ultimate strength of the analyzed concrete specimen. The failure patterns observed under compression loading of confined and unconfined mesoscopic concrete specimens leads to a complete failure that agrees with the experimental result results (Fig. 6).

2.1.1 Confinement Mechanism

The lateral confinement pressure is typically passive in the case of a FRP jacket on concrete. When an axial compression force is applied to FRP confined concrete cylinders, the concrete matrix expands laterally, and the FRP material acts as a barrier, preventing this expansion (Touhari and Mitiche-Kettab 2016).

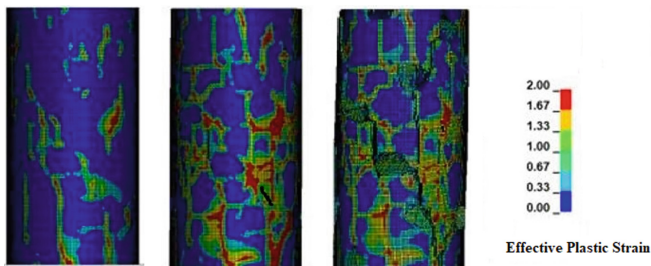


Fig. 4. Unconfined concrete failure patterns

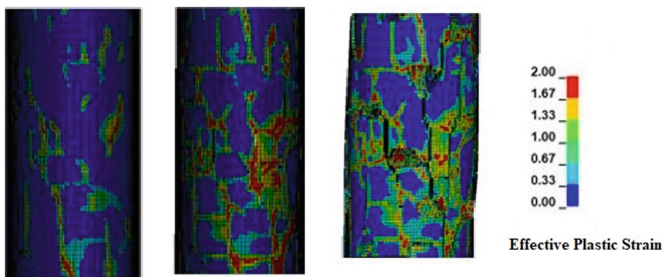


Fig. 5. Confined concrete failure patterns

Confined concrete's mechanical behavior are summarized into two parts: first, it is elastic, which corresponds to low strain levels (Berthet et al. 2006). The elasticity and strain compatibility of the concrete core and composite jacket are the essential components for the relationships that describe the first branch (Berthet et al. 2006). The plastic branch is the second part of this phenomenon. At this point, increased levels of stress are observed (Berthet et al. 2006). Figure 6 plot the maximum effective stress

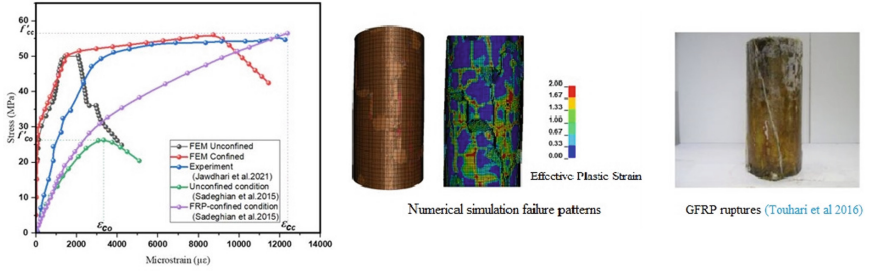


Fig. 6. Static stress-strain curve and failure patterns comparison to the experiment by (Touhari and Mitiche-Kettab 2016)

strain curve of mortar matrix. Firstly, the unconfined stress strain is plotted. Based on the compressive strength of the simulated concrete, the peak value is determined. The plotted curve looks similar to that of the conventional concrete subjected to uniaxial compression test see Fig. 6. Due to the confinement mechanism, the predicted stress-strain curve is in accordance with the experimental results of most confined concrete specimens.

$$f_l = \rho_k \rho_\varepsilon f'_{co} = \frac{2E_f \varepsilon_{h,rupt}}{D} \quad (1)$$

$$\rho_\varepsilon = \frac{2E_f t}{(f'_{co} \varepsilon_{co}) D} \quad (2)$$

$$\rho_\varepsilon = \frac{\varepsilon_{h,rupt}}{\varepsilon_{co}} \quad (3)$$

Assuming that the unconfined concrete strength is equal to f'_{co} , and that the axial strain is equal to $f'_{co} \varepsilon_{co}$, the elastic modulus of the FRP wrap is equal to $k_{eh,rupt}$. The actual rupture strain of the FRP wrap and D is the concrete core diameter. The maximum confinement stress is determined as f_l (Ahmad et al. 2020; Sadeghian and Fam 2015). ρ_k and ρ_ε relationship is governed by Eqs. (1–3) presented by Teng et al. (Lim et al. 2016).

2.2 Concrete's Mechanical Reaction to Dynamic Loading

2.2.1 Stress Wave

Figure 4(a) shows the comparison of the shaped pulse wave deduced from the SHPB simulation to the experimental test. On the basis of the one-dimensional elastic wave concept Eq. (4), a stress pulse balance is achieved when the sum of the transmitted and reflected waves equals the transmitted wave (Bai et al. 2021; Yang et al. 2015).

$$\sigma_i + \sigma_r = \sigma_t \quad (4)$$

where σ_i , σ_r and σ_t are the dynamic stress of the incident, reflected and transmitted wave as can be seen in Fig. 10. The stress equilibrium is achieved by comparing the two waves.

2.2.2 Dynamic Compressive Strength

The peak stress of the stress strain curve (Fig. 8) represents the dynamic compressive strength predicted through numerical simulation and compared to the dynamic compressive strength obtained during the experiment. Following several simulations, it was discovered that the dynamic compressive strength obtained during simulation also increases with increasing strain rate, which is consistent with the experiment (Bai et al. 2021). With an increase in the strain rate, the dynamic compressive strength of the concrete specimen confined with different layers of FFRP jackets also increases.

2.2.3 Definition of Strain Rate for SHPB Simulation

It is well proven that concrete behaves differently under various strain rates (Yang et al. 2015). Because the velocity used in the experiment (Bai et al. 2021) is too high for numerical analysis and results in a significant increase in simulation errors. Therefore, the strain rates obtained during the experiment were divided by the height of the numerical specimen to obtain similar deformation in simulation at identical strain rates. The figure illustrates the comparison of the stress strain generated by the numerical simulation and the experiment test following a single impact at 157 and 149 s^{-1} (Fig. 8). The failure modes of the confined specimen with two, four, and six layers of FRP at various strain rates are depicted in (Figs. 7, 8, 9 and 10).

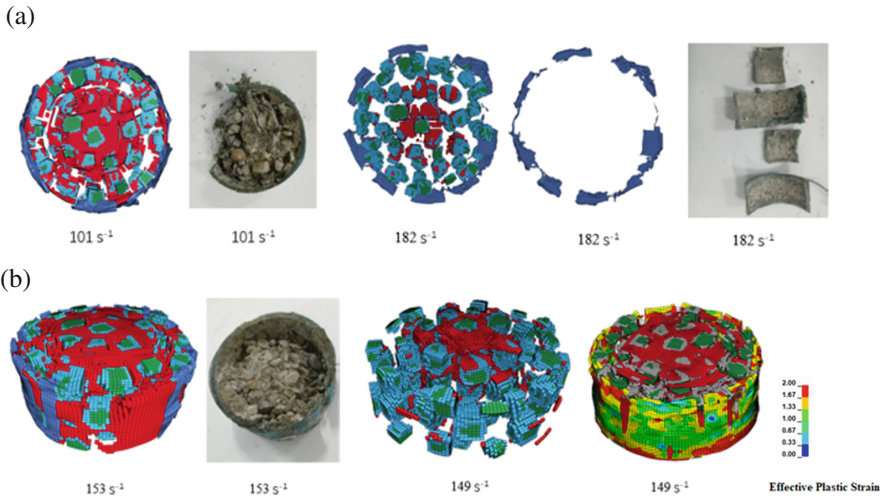


Fig. 7. Typical failure mode of Concrete confined with by FFRP jackets; (a) 2 layers at 101s-1, (b) 4 layers at 182s (c) 6 layers at 153s-1(Bai et al. 2021)

3 Conclusions

For the purpose of investigating the mesoscale behavior of concrete confined by fiber reinforced polymer under static and impact loading, Ls's dyna, which is one of the most

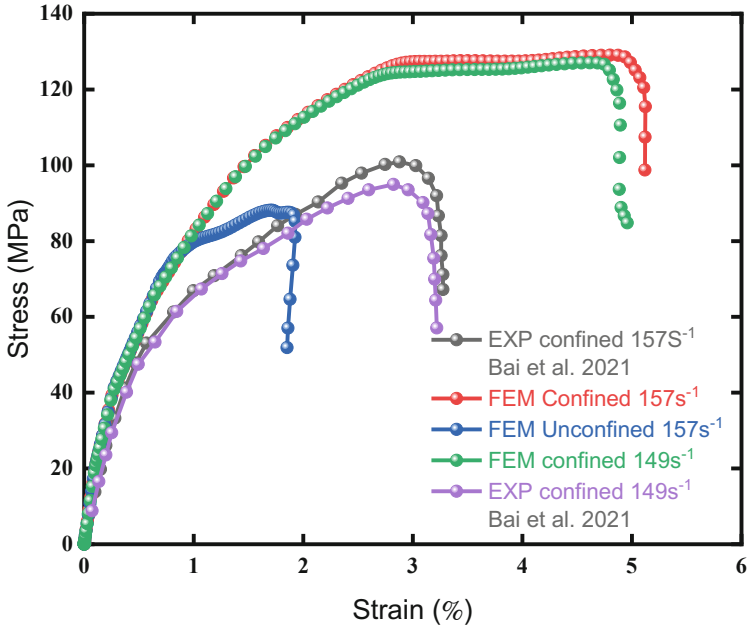


Fig. 8. Stress-strain curve of 6 layers FRP-confined concrete after Impact.

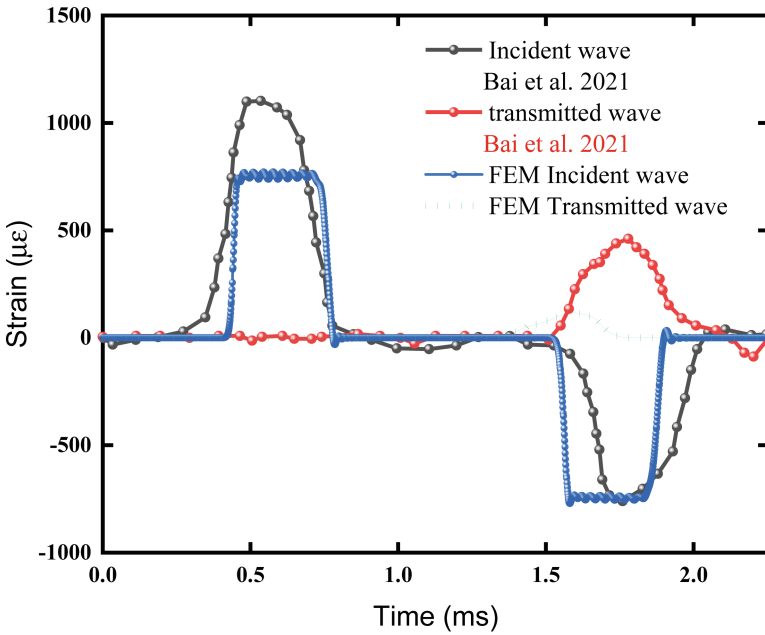


Fig. 9. Typical SHPB waveforms

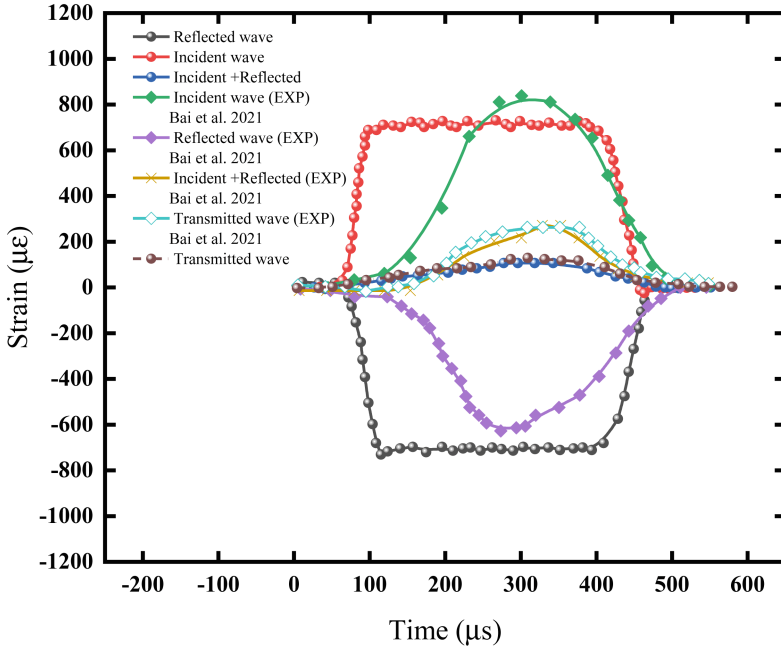


Fig. 10. Incident + reflected wave

widely used finite element modelling software packages, was used in this research to investigate and verify the static and dynamic mechanical responses of confined mesoscale concrete models with glass fiber reinforced polymer for static analysis and flax fiber reinforced polymer for dynamic analysis. The failure mode of FRP-confined concrete as well as the dynamic compression stress-strain curve were investigated, discussed, and compared to experimental test results obtained using the SHPB method. To ensure that the simulation was accurate, other mechanical parameters were examined. These included dynamic compressive strength, strain rate, and the stress wave balance, all of which were used to verify the accuracy of the simulation. As a result, the main conclusion of this work can be briefly summarized as follows:

1. A significant improvement in the strength and toughness of the structure was observed in both dynamic and static tests when the confinement mechanism of glass fiber reinforced polymer and flax fiber reinforced polymer was used on a mesoscale concrete model.
2. Changes in the thickness of the wrapped FRP layer jacket have a significant impact on the confined concrete specimen.
3. Increased strain rate causes a high-velocity wave impact in simulations, resulting in significant concrete damage; the dynamic compressive strength of concrete is defined in accordance with these findings.
4. At remarkably high strain rates simulation, confined concrete performed similarly to unconfined concrete.

References

- Ahmad, A., Plevris, V., Khan, Q.-U.-Z.J.C.: Prediction of properties of FRP-confined concrete cylinders based on artificial neural networks. *10*, 811 (2020)
- Bai, Y.-L., Yan, Z.-W., Jia, J.-F., Ozbakkaloglu, T., Liu, Y.: Dynamic compressive behavior of concrete confined with unidirectional natural flax FRP based on SHPB tests. *Compos. Struct.* **259**, 113233 (2021)
- Berthet, J.F., Ferrier, E., Hamelin, P.: Compressive behavior of concrete externally confined by composite jackets: Part B: Modeling. *Constr. Build. Mater.* **20**, 338–347 (2006)
- Forti, T., Batistela, G., Forti, N., Vianna, N.: 3D mesoscale finite element modelling of concrete under uniaxial loadings. *Materials (Basel)*, **13** (2020)
- Li, X.Q., Chen, J.F., Lu, Y.: Meso-scale modelling of FRP-to-concrete bond behaviour using LSDYNA. In: Ye, L., Feng, P., Yue, Q. (eds.), *Advances in FRP Composites in Civil Engineering*, pp. 494–498. Berlin, Heidelberg. Springer Berlin Heidelberg (2011)
- Lim, J.C., Karakus, M., Ozbakkaloglu, T.: Evaluation of ultimate conditions of FRP-confined concrete columns using genetic programming. *Comput. Struct.* **162**, 28–37 (2016)
- Sadeghian, P., Fam, A.J.E.S.: Improved design-oriented confinement models for FRP-wrapped concrete cylinders based on statistical analyses. **87**, 162–182 (2015)
- Shuguang, L., Qingbin, L.: Method of meshing ITZ structure in 3D meso-level finite element analysis for concrete. *Finite Elem. Anal. Des.* **93**, 96–106 (2015)
- Sathishkumar, T.P., Satheshkumar, S., Naveen, J.: Glass fiber-reinforced polymer composites—A review. *J. Reinforced Plastics Composites* **33**, 1258–1275 (2014)
- Touhari, M., Mitiche-Kettab, R.: Behaviour of FRP confined concrete cylinders: Experimental investigation and strength model. *Periodica Polytechnica Civil Eng.* **60**, 647–660 (2016)
- Wang, J., Jivkov, A.P., Engelberg, D.L., Li, Q.M.: Parametric study of cohesive ITZ in meso-scale concrete model. *Proc. Struct. Integrity* **23**, 167–172 (2019)
- Wu, Z., Zhang, J., Fang, Q., Yu, H., Haiyan, M.: Mesoscopic modelling of concrete material under static and dynamic loadings: A review. *Constr. Build. Mater.* **278**, 122419 (2021)
- Wu, Z., Zhang, J., Yu, H., Ma, H., Fang, Q.: 3D mesoscopic analysis on the compressive behavior of coral aggregate concrete accounting for coarse aggregate volume and maximum aggregate size. *Compos. Struct.* **273**, 114271 (2021)
- Yang, H., Song, H., Zhang, S.: Experimental investigation of the behavior of aramid fiber reinforced polymer confined concrete subjected to high strain-rate compression. *Constr. Build. Mater.* **95**, 143–151 (2015)
- Zhou, X.Q., Hao, H.: Modelling of compressive behaviour of concrete-like materials at high strain rate. *Int. J. Solids Struct.* **45**, 4648–4661 (2008)